A model for heat flow in deep borehole disposals of high-level nuclear waste

Fergus G. F. Gibb,[1] Karl P. Travis,[1] Neil A. McTaggart,[1] and David Burley[1]

Received 20 March 2007; revised 1 November 2007; accepted 21 January 2008; published 6 May 2008.

[1] Deep borehole disposal (DBD) is emerging as a viable alternative to mined repositories for many forms of highly radioactive waste. It is geologically safer, more secure, less environmentally disruptive and potentially more cost-effective. All high-level wastes generate heat leading to elevated temperatures in and around the disposal. In some versions of DBD this heat is an essential part of the disposal while in others it affects the performances of materials and waste forms and can threaten the success of the disposal. Different versions of DBD are outlined, for all of which it is essential to predict the distribution of temperature with time. A generic physical model is established and a mathematical model set up involving the transient conductive heat flow differential equation for a cylindrical source term with realistic decay. This equation is solved using the method of Finite Differences. A Fortran computer code (GRANITE) has been developed for the model in the context of DBD and validated against theoretical and other benchmarks. The limitations of the model, code, input parameters and data used are discussed and it is concluded that the model provides a satisfactory basis for predicting temperatures in DBD. Examples of applications to some DBD scenarios are given and it is shown that the results are essential to the design strategy of the DBD versions, geometric details and choice of materials used. Without such modeling it would be impossible to progress DBD of nuclear wastes; something that is now being given serious consideration in several countries.

Citation: Gibb, F. G. F., K. P. Travis, N. A. McTaggart, and D. Burley (2008), A model for heat flow in deep borehole disposals of high-level nuclear waste, *J. Geophys. Res.*, *113*, B05201, doi:10.1029/2007JB005081.

1. Introduction

[2] There is widespread agreement throughout the scientific community and the international nuclear industry that high-level radioactive wastes (HLW), including spent nuclear fuel (SNF) and fissile materials such as Pu, should eventually be dealt with by geological disposal. Many countries are looking to disposal in geologically shallow (300–800 m), mined and engineered repositories. Such repositories may be "wet" or "dry" [*Gibb*, 2005]. "Wet" repositories are below the water table in the zone of near-surface groundwater circulation and may be in "crystalline" (i.e., igneous or metamorphic) rocks like granite, as proposed in Sweden, Finland and Canada, or sedimentary rocks like shale and clay as currently favored in Switzerland, France and Belgium. "Dry" repositories may be above the contemporary water table (e.g., Yucca Mountain, Nevada) or in evaporite formations (e.g., the Waste Isolation Pilot Plant, New Mexico). As is well known, mined repositories are not without their problems: geological, technical and otherwise. However, a potentially superior solution is "deep" disposal in large diameter boreholes drilled 4–5 km into the granitic basement of the continental crust. This is variously referred to as deep borehole disposal (DBD) or very deep disposal (VDD), the latter distinguishing it from mined repositories, which are sometimes referred to as deep (in engineering terms) disposal. The idea of disposing of radioactive wastes in deep boreholes has been around since at least the 1950s [*Chapman and Gibb*, 2003] but it is only the great advances in scientific and commercial deep drilling technology over the last two decades that have made VDD in boreholes a realistic proposition.

[3] Deep boreholes offer many advantages over mined repositories [*Gibb*, 1999, 2000; *Chapman and Gibb*, 2003; *Ansolabehere and Deutch*, 2003; *Gibb et al.*, 2008b], especially in the areas of safety, cost, environment, site availability, security, longevity, insensitivity to waste type and flexibility of commitment. The greater safety arises from the geological barrier (to any return of radionuclides to the biosphere) being an order of magnitude greater and the bulk hydraulic conductivities for intrarock fluid flow usually being extremely low at such depths. Particularly significant in the safety context are the density-stabilized, stratified brine intrarock fluids that, at such depths, have usually been physically and chemically isolated from the near-surface groundwaters for many millions of years and are likely to remain so far into the future. Hence any radionuclides escaping from the primary containment into these fluids will go effectively nowhere in a million years.

[1] Immobilisation Science Laboratory, Department of Engineering Materials, University of Sheffield, Sheffield, UK.

0148-0227/08/2007JB005081$09.00

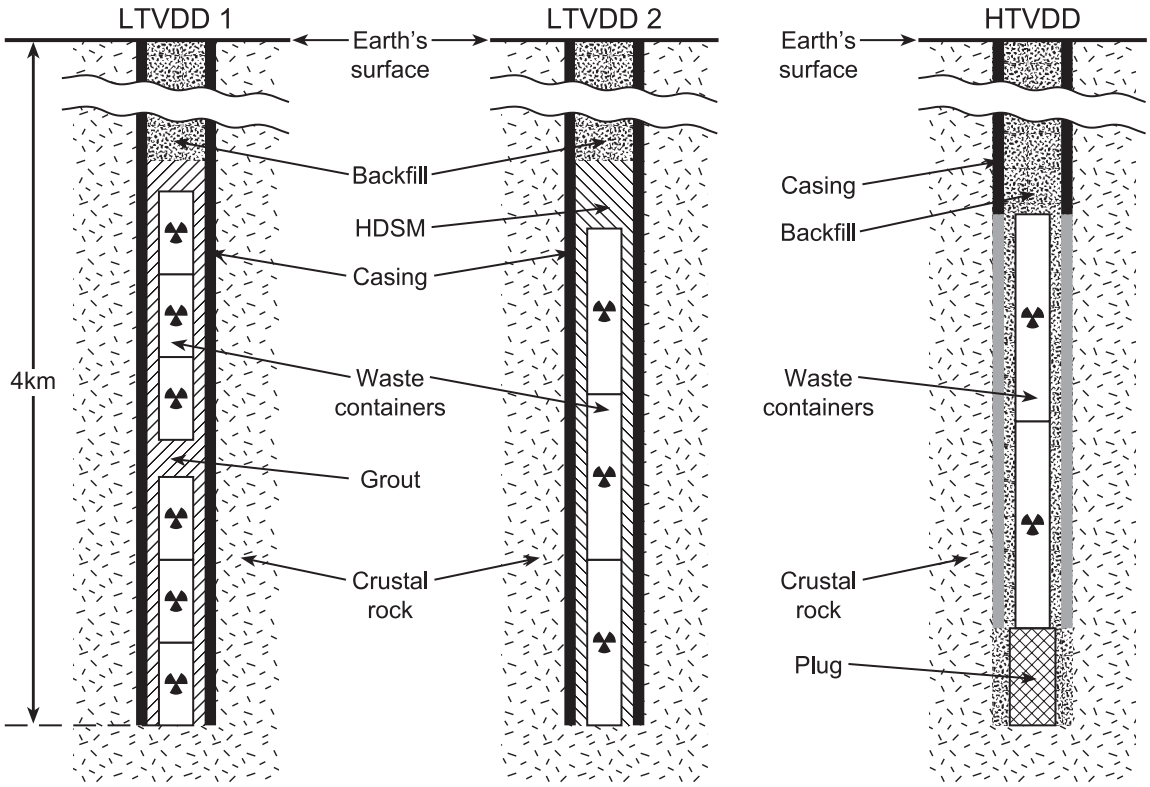

Figure 1. Three versions of deep borehole disposal (LTVDD = low-temperature very deep disposal, HTVDD = high-temperature very deep disposal, HDSM = high-density support matrix).

Since the cost of a 4 km deep borehole large enough to dispose of upwards of 250 m^3 of HLW is around US$7 M [*Harrison*, 2000] (adjusted to 2007 values), the cost of disposal of equivalent amounts of HLW should be one to two orders of magnitude less for borehole VDD than for a mined repository (Yucca Mountain is projected to cost >US$49 B). Deep boreholes are much less environmentally disruptive than mined repositories. Physical damage to the rock rarely extends more than a fraction of the borehole radius beyond the wall and, since many boreholes can be sunk from a closely spaced set of wellheads [*Chapman and Gibb*, 2003], the surface area required by the drilling rig and other facilities can be considerably less than 1 km^2. Also, once the last borehole is filled and sealed the surface site can be restored to pristine green-field condition. The only geological requirement of the site is relatively unfractured granitic rock between 2 and 5 km depth with bulk hydraulic conductivities less than about 10^{-10} m s^{-1}. Since this applies to a substantial portion of the continental crust there should be no shortage of geologically suitable sites in most countries. Any storage or disposal of HLW, especially fissile materials like Pu, raises concerns about security, principally vulnerability to terrorist attack and illegal misappropriation. HLW in deep boreholes beneath 3 or 4 km of granite is about as secure as it can be and could certainly survive any conceivable terrorist attack. Also, any recovery would be a major engineering feat and certainly could not be done quickly or covertly. In contrast to mined repositories in which reliance on the near-field engineered barriers predominates over the far-field geological barrier, VDD in boreholes makes maximum use of the geological barrier – the only one that can demonstrably survive on a timescale of millions of years. VDD is relatively insensitive to the type and composition of the waste other than that it should be solid. Because of the depth and the high confining pressures (~150 MPa) even normally volatile radionuclides, such as ^{129}I, would not escape the containment. Finally, a program of VDD in boreholes offers flexibility of commitment in that the number of holes can vary from one upwards and be terminated at any point if waste management requirements change without significant loss of capital investment. All of the above should make borehole VDD more acceptable to political and regulatory authorities, the nuclear industry and the public.

[4] The only argument against VDD is the enormous difficulty and expense of any attempt to retrieve the waste. However, there is little scientific or technical justification for retrievability [*Gibb*, 2006] – indeed, in the security context it would be highly undesirable.

2. Very Deep Disposal Versions

[5] We are currently investigating and developing four main versions of borehole VDD [*Gibb et al.*, 2008a, 2008b], each designed for a different category of HLW (Figure 1). The first three are variants of low-temperature very deep disposal (LTVDD) for moderate heat generating waste forms while the fourth is a high-temperature very deep disposal (HTVDD) scheme that requires the waste to have sufficient heat output to partly melt the enclosing rock.

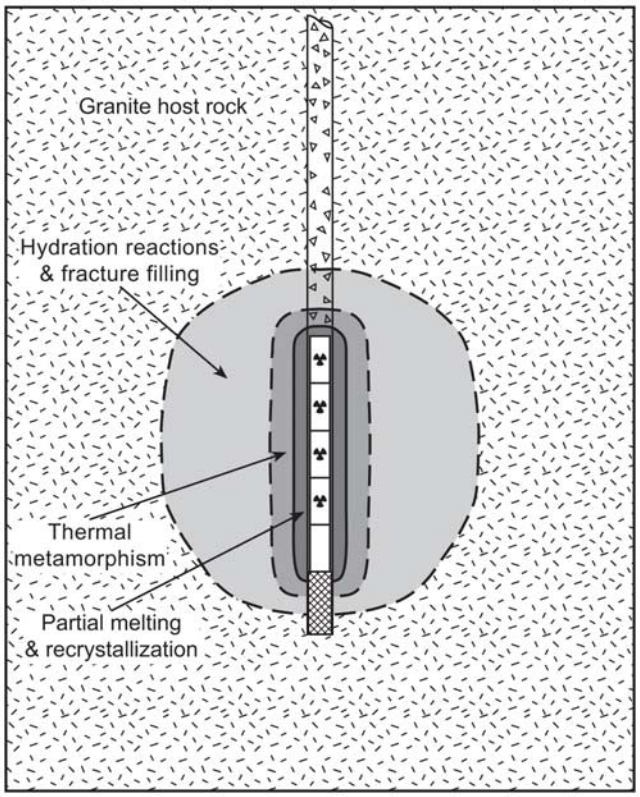

Figure 2. Schematic of high-temperature very deep disposal (HTVDD). Zones not to scale.

[6] LTVDD-variant 1 is for HLW packages with a specific gravity less than ~4, such as cylindrical stainless steel containers filled with vitrified reprocessing waste similar to those produced at the Waste Vitrification Plant at Sellafield in the UK and elsewhere. The packages are deployed singly or in batches (of a few containers) over the lowermost 1 km or so of a fully cased borehole sunk into granitic rock. The steel casing is perforated to reduce weight and to enable fluid access between the interior and the wall rock. Following the emplacement of each container or batch an appropriate grout or cement is pumped down the hole to fill the space between the containers and casing and any gaps between the casing and wall rock, displacing any borehole fluid in the process. When the container or batch is completely encased in a cocoon of grout the material is allowed to set hard, enabled or facilitated by heat from the waste, before the next batch of containers is deployed. When the deployment of waste packages is complete the hole above the deployment zone is backfilled with crushed host rock and permanently sealed at intervals to ensure there is no possible fluid flow path back up the borehole. The sealing could be accomplished using one or more of several materials and methods but perhaps the ideal would be "rock welding" through partial melting and recrystallization of the backfill and wall rock [*Attrill and Gibb*, 2003a, 2003b]. This could be achieved using special containers filled with high heat generating radioactive waste (see HTVDD below) or, more simply, by electrical downhole heating.

[7] LTVDD-variant 2 is designed for the disposal of waste packages of relatively high specific gravity, such as containers packed with spent nuclear fuel rods (SNF) that have undergone a prolonged period of post-reactor cooling embedded in an appropriate matrix, such as Pb or glass. For UO_2 fuels such packages would have specific gravities between 8 and 11 and be deployed in longer containers and stacks than in variant 1. Instead of the cementitious grout used in variant 1, a special Pb-based alloy, high-density support matrix (HDSM) is deployed as a fine shot to surround the containers [*Gibb et al.*, 2008a]. Within a few weeks of emplacement, the decay heat from the containers melts the HDSM, which remains partly molten for several decades before solidifying to effectively 'solder' the waste packages into the borehole. The main function of the HDSM is to render the packages only slightly less than neutrally buoyant, thus eliminating any risk of container deformation and failure as a consequence of excessive vertical load stresses, but it also confers many safety and other benefits [see *Gibb et al.*, 2008a]. Post-deployment backfilling and sealing of the borehole are the same as for variant 1.

[8] LTVDD-variant 3 is intended for the disposal of plutonium and other actinides and makes use of smaller (~0.3 m), deeper (>6 km) boreholes. Since heat outputs of the specialized wasteforms and consequent temperature effects on the enclosing rock are relatively small, the requirement for heat flow modeling is substantially less and this version does not feature further here.

[9] HTVDD involves the deployment of special containers of high heat generating waste in the lowermost part of the borehole [*Gibb*, 1999, 2000; *Gibb and Attrill*, 2003; *Gibb et al.*, 2008b]. Potentially suitable HLW could be relatively undiluted reprocessing waste or SNF after less than ~5 years post-reactor cooling (varying with type and burn-up). Depending on factors such as the thermal loading of the containers, the packages may be deployed singly or in batches. After each deployment the casing around the packages may (Figure 1) or may not [*Gibb et al.*, 2008b] be withdrawn. The spaces between the containers and wall rock are then filled with an aqueous slurry of crushed granite to ensure good thermal conductivity between the containers and the host rock. The radioactive decay heat from the HLW gradually generates temperatures in and around the waste package(s) greater than 700°C, which are sufficient to cause partial melting of the host granite under the prevailing high pressure conditions at ~4 km depth in the continental crust [*Attrill and Gibb*, 2003a]. As the heat output of the HLW declines these partial melts cool slowly enough to enable complete recrystallization [*Attrill and Gibb*, 2003b] so sealing the waste packages into a sarcophagus of solid granite, surrounded by zones of thermal metamorphism in which any pre-existing fractures are sealed by solid-state recrystallization, annealing and hydration mineralization (Figure 2). The waste is thus entombed in a robust, multibarrier, near-field containment complementing the immense far-field geological barrier to give potentially the safest and most durable containment possible.

3. Temperature Modeling

[10] For all versions of borehole VDD it is essential to be able to predict accurately the distribution of temperature in

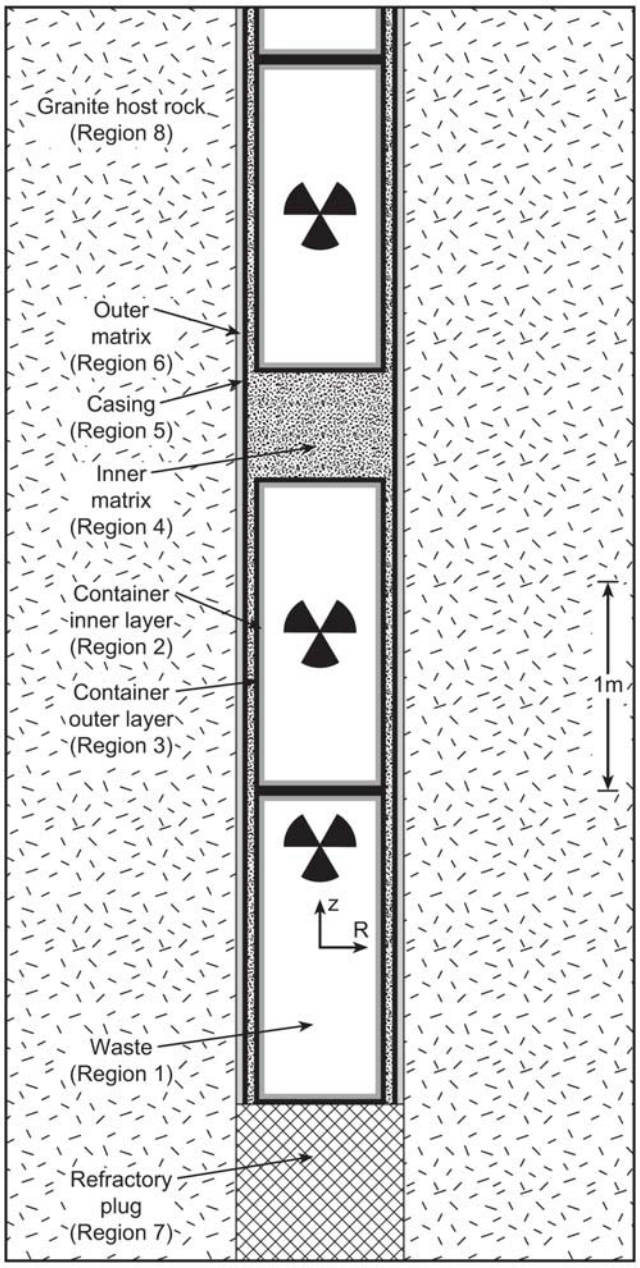

Figure 3. Generic physical model as used for mathematical modeling.

and around the HLW packages as a function of time and as a consequence of the decay of the waste, at least until such time as it has a negligible effect on the ambient temperature. For some HLW types and disposal geometries it has been implied that this could be up to 10^4 years [e.g., *Hodgkinson*, 1977]. At depths of 4 to 5 km in the continental crust the ambient temperature varies according to the local geothermal gradient but can be in excess of 100°C, especially where geologically young bodies of granite are involved.

[11] For LTVDD, knowledge of the temperature/time distribution is crucial to performance assessments of all components of the near-field containment such as the wasteform, container, grout or HDSM and casing. It is also essential for predicting the likely thermal effects on the adjacent host rock and calculating the extent of any thermally induced perturbations in the intrarock fluid system.

[12] In HTVDD it is of much less consequence what becomes of the waste and its packaging once they are sealed into their coffin of recrystallized granite. It is worth noting here that this is likely to occur within a few decades at most after deployment [*Attrill and Gibb*, 2003b; *Gibb et al.*, 2008b]. The temperature/time distribution around the waste packages determines the extent, geometry and formation kinetics of the zone of melting and recrystallization, all of which can be predicted by combining the results of temperature/time modeling with experimental data on melting and recrystallization [*Attrill and Gibb*, 2003a, 2003b]. Consequently, knowledge of the temperature/time distribution in the host rock around the borehole is crucial for this type of disposal and is also important for calculating the extent of any effects that transient elevation of the ambient temperature might have on the intrarock fluid system. The latter might become significant in the unlikely event of any radionuclides escaping from the granite sarcophagus in the short term, i.e., prior to return to near-ambient temperatures.

[13] This paper describes a mathematical model and computer code for predicting the distribution of temperature with time in and around very deep disposals of heat-generating wastes in boreholes. It is based on a generic physical model in which variation of key parameters allows correspondence to each of the VDD versions. Having established the model the paper goes on to focus on validation and the constraints and limitations inherent in its use before giving some examples of its applications. A complementary paper [*Gibb et al.*, 2008b] describes a series of case studies in which the numerical outcomes from the model are used to demonstrate the viability of different versions of LTVDD and HTVDD.

4. Physical Model

[14] For modeling purposes we require a single generic model with sufficient flexibility to accommodate the differences between the various versions of VDD and allow the use of realistic ranges of possible configurations, materials and physical properties. This model is illustrated in Figure 3 and its main features are as follows.

[15] The diameter of the borehole is variable up to 1 m (and beyond if necessary). The casing, which may be present or absent, can be of any outer diameter (up to the borehole diameter) and wall thickness and made of any material. The containers are cylindrical, of variable diameter, wall thickness and length, and can consist of more than one layer, each of which can be made from any material. The contents of the containers and their heat outputs and decay rates can be varied, although these are assumed to be uniform within each container. The material between the wall rock and casing (outer matrix, Figure 3) and between the casing and containers (inner matrix, Figure 3) can be the same or different. Containers can be emplaced singly or in variable stacks with vertical spacers between stacks, which may be of the same (matrix) material or different. The relevant thermal and physical properties of all materials are variable and can incorporate temperature dependence. Because the pressure dependencies of the properties of most of the materials involved are poorly known, and wherever one is, it tends to be relatively insignificant over the 0–150 MPa

range, pressure effects are ignored at present. Note that the refractory base plug in Figure 3 is an essential component only in the HTVDD version.

5. Mathematical Model

[16] To investigate the time-dependent temperature profile in the near and far field environments we have constructed a mathematical model of the conductive heat energy transfer occurring in the proposed disposal scenarios. This model allows us to experiment easily with different configurations, materials, thermal properties and decay rates without the need for time-consuming and expensive laboratory experiments. An additional advantage of a mathematical model is that it enables prediction of the temperature evolution over a wide range of timescales from seconds to millennia.

[17] Our model is constructed by taking a heat energy balance over each region of material in our disposal scenario, including the waste region, container material, backfill, borehole casing and finally, the surrounding rock.

[18] When heat is transferred by conduction alone, the temperature in a given region changes with time according to

$$\rho c \frac{\partial T}{\partial t} = \nabla \cdot (K \nabla T) + S \tag{1}$$

where ∇ is the usual spatial gradient operator, K is the thermal conductivity of the material, ρ its density, c its specific heat and S represents the source term (the heat output per unit time per unit volume). The above form of (1) is quite general and thus in our disposal problem the source term will be non-zero in the region enclosing the heat generating radioactive waste only.

[19] To simplify the model we assume each material to be homogeneous and that the engineered materials have uniform shape and a high degree of symmetry. In practice, this will not be the case (see 8.1.1); for example the containers may not be perfectly cylindrical, and may have a lip, taper or bevel engineered into their design. These are minor details which, if necessary, could be incorporated into our model at a later stage. For a container which is taken to be a perfect cylinder, the mathematical problem can be simplified by changing from a Cartesian coordinate system to a cylindrical one in which a point is described respectively by the radial, axial and angular coordinates, (R, z, θ). In this coordinate system, (1) becomes

$$\frac{1}{R}\frac{\partial}{\partial R}\left(\kappa R \frac{\partial T}{\partial R}\right) + \frac{\partial}{\partial z}\left(\kappa \frac{\partial T}{\partial z}\right) = \frac{\partial T}{\partial t} - \frac{S}{\rho c} \tag{2}$$

in which there is no dependence on the angle θ as a result of the axial symmetry and κ is the thermal diffusivity $(K/\rho c)$. In general the thermal conductivity may be a function of the spatial coordinates and the temperature of the material. In our model we take K to be piecewise constant. In other words, within each of the regions in which (2) is solved, K is taken to be independent of the spatial coordinates.

[20] We are interested in calculating the instantaneous temperature rise, $\bar{T}(R, z, t) = T - T_0$, as a function of the radial and axial positions. This quantity may in principle be obtained from the solution of (2). In practice, no analytical solution can be found for the general case involving a time dependent source term and variable thermal properties. However, (2) is readily solved using well established numerical methods. A number of commercial software packages exist for solving all or part of this work including: process simulation codes, finite element codes and computational fluid dynamics software. Such packages are not designed to allow the user to develop the source code which can be a disadvantage when employed in fundamental research work. We have therefore chosen to develop our own (finite difference) code for solving the heat conduction problem with a view to incorporating new developments quickly and efficiently, and to interface with other modeling methodologies to develop, ultimately, a true multiscale modeling package.

[21] One numerical strategy for solving (2) is to replace the differential operators by finite difference operators, giving rise to a system of algebraic equations to solve on a spatial grid (mesh) for a set of discrete times. This is known as the method of Finite Differences (FD).

[22] To solve (2) by FD we first break up the solution space into different regions, each governed by different thermal properties. The different regions in the problem domain for the general case are indicated in Figure 3. A particular disposal scenario may contain all 8 different regions or it may contain fewer. For example, only in the case of the HTVDD scheme is it necessary to include region 7. In all other cases the zone below the container will be replaced by a continuation of the rock (region 8). The source term is associated with region 1 only. A rectangular mesh is then created using a non-uniform spacing; a finer spacing is employed in the near field environment, while a wider spacing applies further away from the container(s). The origin of the mesh is then placed along the axis of symmetry at a point mid-way up the first waste container. Labeling successive points along the mesh parallel to the radial axis as i, $i + 1$, etc. and those points which run parallel to the z axis as j, $j + 1$, etc. we may discretize (2) to give

$$\begin{aligned}
&\frac{1}{R\left(i+\frac{1}{2}\right) - R\left(i-\frac{1}{2}\right)} \frac{1}{R(i)} \begin{bmatrix} \kappa\left(i+\frac{1}{2},j\right) R\left(i+\frac{1}{2}\right) \left\{\frac{T(i+1,j)-T(i,j)}{R(i+1)-R(i)}\right\} \\ -\kappa\left(i-\frac{1}{2},j\right) R\left(i-\frac{1}{2}\right) \left\{\frac{T(i,j)-T(i-1,j)}{R(i)-R(i-1)}\right\} \end{bmatrix} \\
&+ \frac{1}{z\left(j+\frac{1}{2}\right) - z\left(j-\frac{1}{2}\right)} \begin{bmatrix} \kappa\left(i,j+\frac{1}{2}\right) \left\{\frac{T(i,j+1)-T(i,j)}{z(j+1)-z(j)}\right\} \\ -\kappa\left(i,j-\frac{1}{2}\right) \left\{\frac{T(i,j)-T(i,j-1)}{z(j)-z(j-1)}\right\} \end{bmatrix} \\
&= \frac{1}{\Delta t}\left[T^{t+\Delta t}(i,j) - T(i,j)\right] - \frac{S(t)}{\rho c}
\end{aligned} \tag{3}$$

where Δt is the time step size, $T(i, j)$ is the temperature at the current time at mesh point (i, j), while $T^{t+\Delta t}(i, j)$ is the temperature at the same mesh point at the later time of $t + \Delta t$. The first term of the left hand side of (3) is the discretized equivalent of $(1/R)\partial/\partial R(\kappa R \partial T/\partial R)$ while the second term on the left hand side is a discretization of $\partial/\partial z(\kappa \partial T/\partial z)$. Note that the quantities κR (thermal diffusivity multiplied by radial position) and κ are evaluated at the midpoints of each pair of nodes used to evaluate the derivatives. For a mesh consisting of n divisions along the radial direction and m divisions along the axial direction

the set of $n \times m$ equations in (3) may be written in a more compact manner employing matrices

$$\boldsymbol{A}\boldsymbol{T}^{t+\Delta t} = \boldsymbol{B}\boldsymbol{T} + \boldsymbol{S} \tag{4}$$

where $\boldsymbol{T}$ and $\boldsymbol{T}^{t+\Delta t}$ are now column vectors containing the temperatures for the whole set of mesh points at the present time and the new time respectively, $\boldsymbol{A}$ and $\boldsymbol{B}$ are square matrices of dimension $n \times m$ that contain all the physical and geometrical parameters, while $\boldsymbol{S}$ contains the contribution from the source and some of the boundary conditions. In this formulation, usually called the explicit form for the equations, the matrix $\boldsymbol{A}$ is diagonal. The computations are simple but there is a severe limitation on the time step otherwise instability occurs.

[23] To avoid this limitation the temperatures on the right hand side of the matrix equation are written:

$$(1-\alpha)\boldsymbol{T} + \alpha\boldsymbol{T}^{t+\Delta t} \qquad \text{where} \qquad 0 \le \alpha \le 1 \tag{5}$$

[24] The case $\alpha = 0$ recovers the explicit formulation while $\alpha = 1/2$ and $\alpha = 1$ give the common implicit cases; Crank-Nicolson and fully implicit respectively. We have used a fully implicit method in our computer code.

[25] There is no restriction on the time step for the stability of implicit computations but the accuracy deteriorates as the time step increases, so care was taken to check on accuracy. In both fully implicit and Crank-Nicolson cases the matrix equation is reformulated and $\boldsymbol{A}$ is no longer diagonal. This necessitates the use of a matrix solver. However, the matrix is still sparse (it is 5-diagonal) and efficient algorithms exist for such systems of equations. In this work we employed a lower/upper decomposition method with iterative refinement.

[26] The form of (3) is quite general and may be used in cases where the thermal conductivity depends on the spatial coordinates, e.g., across the regions in the model. In our code we have a thermal conductivity which is piecewise constant (which is obviously true for the thermal diffusivity as well) and in that case, the κ in (3) are simply evaluated at the same nodes as used to evaluate the derivatives. However, care must be taken at an interface. At mesh points which reside on an interfacial boundary we use the midpoint values of the thermal conductivity.

[27] All the physical parameters, K, ρ, c, S may be time dependent and/or temperature dependent. This causes no problem to the formulation since they are all varying very slowly so that their values at the current time t may be used and they can be updated at the new temperatures after the time step is completed.

[28] When melting and solidification of one or more of the materials (e.g., HDSM in LTVDD-2 or host rock in HTVDD) take place a new modeling problem occurs. Clearly, heat is extracted during melting and released during crystallization to satisfy the latent heat requirements of the process and these have an effect on the amount of heat conducted. The exact natures of these processes, which occur over a range of temperature (the solidus – liquidus interval), are not well defined, especially for the complex phase assemblage of the natural granite host rock. Not only are the values of latent heat for complete melting poorly constrained but the absorption/release of energy through the solidus – liquidus interval is unknown (see section 8.3.5). Consequently, the approach adopted in our model is to consider the two bounding cases, one in which no latent heat is involved and the other in which all the latent heat is released/absorbed at the solidus temperature. Phase changes also have the potential to affect the modeling in other ways. Physical properties, such as thermal conductivity, may change but, as we are unaware of any such data for partly melted granite for example, we have no option but to ignore this in the modeling. Also, the generation of liquid phases in the system introduces the possibility of heat transfer by convection (see discussion below). However, at least in the case of granitic partial melts, these liquids will be so viscous that this possibility can be disregarded as far as the modeling of heat transfer is concerned.

[29] The mathematical model is completed by the specification of the boundary conditions. These take the form: (1) the conditions at the axis are that the temperature remains finite and that there is zero flux across this boundary $K\partial T/\partial R = 0$ at $R = 0$; (2) at large distances from the source the temperature rise is set to be zero (alternatively set the absolute temperature to the ambient value); (3) at inter-regional boundaries it is ensured that the temperature and flux are the same on either side of the boundary; and (4) the initial condition takes a zero (or ambient) temperature over all spatial regions. (In dealing with problems involving multiple containers in which additional containers are added sequentially, the current temperature distribution at the time a new container is fed in is taken to be the new initial condition).

6. Computer Code (GRANITE)

[30] A computer code, written in Fortran 90, has been developed for solving the heat flow problem defined in 5. This code has been named GRANITE (not to be confused with the rock granite). Fortran was chosen because it is a language designed for computationally intensive floating point calculations and many efficient subroutines are available for solving systems of linear equations such as the NAG libraries. We envisage adding a graphical user interface to the eventual GRANITE package and for this we will use the Perl Tk language.

[31] The code has been designed to treat a wide range of specific problems pertaining to the DBD/VDD concept. There is flexibility for setting up the FD mesh, the form of the source term and establishing a multilayered disposal scenario in which each layer can have different physical and thermal properties. Further, although the code is designed to model single boreholes with single or multiple containers, it could be modified to model scenarios where several boreholes are sunk close together. A realistic nuclear waste disposal campaign would involve the emplacement of containers in batches, with a time delay between each batch. This scenario has also been built into GRANITE. Other key features of the code are described below.

6.1. Mesh Creation

[32] A rectilinear mesh is generated which represents a two dimensional vertical slice through the axisymmetric physical system. This mesh is superimposed on the borehole

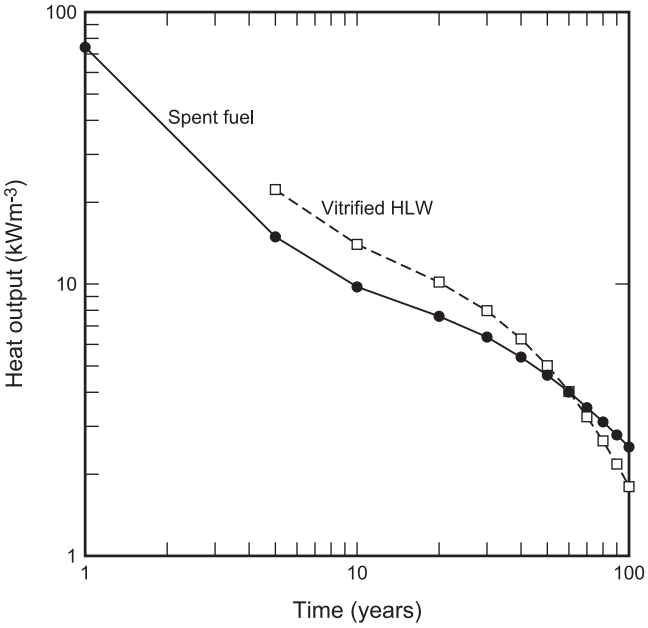

Figure 4. Thermal decay data calculated by FISPIN for a typical reprocessing waste (3:1 blend of 40GWd/t LWR and 5 GWd/t MAGNOX) and 45GWd/t PWR spent fuel.

such that the left hand edge of the mesh coincides with the borehole axis and the right hand edge is out in the surrounding rock. Different material properties are assigned to different mesh points. For example, those points lying inside the containers have the properties of waste (SNF or vitrified waste), points lying at or beyond the borehole radius have the properties of rock, etc. In this way different thermal properties are applied to each mesh point according to the physical region (material) in which it lies.

6.2. Sequential Insertion

[33] The mesh file contains all the information required so that the code can simulate container insertions. The only user variable is the insertion interval, i.e., how often a new container is deployed in the borehole. The idea is that certain points in the borehole may initially have thermal properties of the borehole filling (fluid). Then, to simulate the addition of a new container to the top of the stack already in the borehole, a specified set of points have their thermal properties switched from those of the fluid to those of waste, etc. This assumes the instantaneous arrival of the new container in the borehole. Of course, in reality, a new container takes a finite time to arrive in position from the top of the borehole, realistically around a day. However, the thermal response time of the disposal environment is low compared to the insertion time, so the assumption of an instantaneous arrival makes little difference to the temperature solution.

6.3. Generation of Isotherms

[34] GRANITE calculates the temperature at every mesh point at pre-set time steps over a specified duration. At selected times during this iteration process the instantaneous temperature solution is stored and used to define a set of isotherms for that time solution. These isotherms therefore represent a snapshot of the thermal environment of the borehole. A large number of such snapshots can be generated for inspection, viewing as an animation or the creation of more sophisticated isotherm diagrams, such as isotherms of the maximum temperatures reached (irrespective of the time taken to attain them). This last facility is especially useful for evaluating the performance of materials used in the disposal and determining the extent of the zone of partial melting in HTVDD, i.e., the dimensions of the granite sarcophagus (see section 11.3).

6.4. Decaying Heat Sources

[35] Different types of spent nuclear fuel and reprocessing wastes are complex cocktails of different isotopes with a wide range of half lives. For reprocessing wastes the main heat generators when the waste is relatively new are the fission products like ^{144}Pr, ^{90}Y and ^{134}Cs but after 10 years or so the main contributors are actinides like ^{241}Am, ^{244}Cm and ^{243}Am with some longer lived fission products like ^{137}Cs and ^{90}Sr. Spent fuel normally undergoes a period of post-reactor cooling so that by the time it might be disposed of the main contributions to heat generation come from the likes of ^{90}Y, ^{137M}Ba, ^{137}Cs, ^{90}Sr and ^{238}Pu. Heat decay data for an actual vitrified reprocessing waste and a typical LWR spent fuel have been calculated for a meaningful set of ages (Figure 4) using the nuclear industry's standard code, FISPIN [*Burstall*, 1979]. The actual decay curves are complex and cannot be fitted by any simple analytical form. Consequently, we have used straight line interpolations between the data points in Figure 4 to feed into GRANITE where the heat is recalculated at every time step (see section 8.3.4). The errors inherent in this approach are so small that they would not be significantly reduced by FISPIN calculations at shorter intervals.

6.5. Boundary Conditions

[36] On the left edge of the mesh (borehole axis) the boundary condition is adiabatic (zero flux). On the other three edges of the mesh the boundary condition is Dirichlet, i.e., constant temperature set at ambient conditions (see section 8.2.1). A development under consideration is the use of line source calculations to derive temperature solutions for distances far away from the borehole. These could replace the present ambient temperature boundary conditions allowing the mesh edges to be brought nearer to the borehole without sacrificing solution accuracy and so give smaller meshes and reduce computing demands (see section 8.2).

7. Validation of the GRANITE Code

[37] In order to ensure that the code is producing sensible results we have validated it against a number of simple, well defined examples in heat conduction which have analytical or semi-analytical solutions. Each of these cases can be built from a very useful construct, namely the temperature rise due to an instantaneous point source of heat.

[38] For the case of constant thermal diffusivity and zero source term, the heat conduction equation (1) becomes

$$\frac{\partial^2 T}{\partial x^2} + \frac{\partial^2 T}{\partial y^2} + \frac{\partial^2 T}{\partial z^2} = \frac{1}{\kappa}\frac{\partial T}{\partial t} \tag{6}$$

A particular solution of (6) is

$$\bar{T} = \frac{Q}{8(\pi\kappa t)^{3/2}} \exp\left\{-\left[(x-x')^2+(y-y')^2+(z-z')^2\right]/4\kappa t\right\}, \tag{7}$$

which can be regarded as the temperature rise due to a point source which supplies a quantity of heat, $Q\rho c$, generated at the point (x', y', z') at $t = 0$ [*Carslaw and Jaeger*, 1959]. From this basic result the temperature rise due to an instantaneous line source supplying a quantity of heat $Q_L\rho c$ per unit length at $t = 0$, parallel to the z axis and passing through the point (x', y') may be derived by integrating (7) over the z coordinate (the line can be considered to comprise a series of uniformly distributed point sources each supplying a quantity of heat $Q_L\rho c dz'$ located at z'). The solution is

$$\begin{aligned}\bar{T} &= \frac{Q_L}{4\pi\kappa t} \exp\left[-\left\{(x-x')^2+(y-y')^2\right\}/4\kappa t\right] \\ &= \frac{Q_L}{4\pi\kappa t} \exp\left(-R^2/4\kappa t\right),\end{aligned} \tag{8}$$

where the final equality follows from the introduction of polar coordinates ($R^2 = (x - x')^2 + (y - y')^2$).

7.1. Single Continuous Point Source of Heat

[39] The temperature due to a point source located at the point (x', y', z') which is supplying heat at a rate, $\phi(t)\rho c$ from $t = 0$ to $t = t$, may be obtained by integrating (7) with respect to time, giving

$$\bar{T} = \frac{1}{8(\pi\kappa)^{3/2}} \int_0^t dt' \frac{\phi(t')}{(t-t')^{3/2}} \exp\left\{-r^2/[4\kappa(t-t')]\right\} \tag{9}$$

where the relation $r^2 = (x - x')^2 + (y - y')^2 + (z - z')^2$ has been used to simplify the equation.

[40] The integral in (9) cannot be written explicitly for most $\phi(t)$ and requires numerical integration. However, for a constant source $\phi(t) = q$, the integration can be performed analytically to give

$$\bar{T} = \frac{q}{4\pi\kappa r} erfc\left(\frac{r}{\sqrt{4\kappa t}}\right) \tag{10}$$

where $erfc(x)$ is the complementary error function defined by

$$erfc(x) = \frac{2}{\sqrt{\pi}} \int_x^\infty e^{-s^2} ds. \tag{11}$$

[41] Since $erfc(0) = 1$, in the limit $t \to \infty$, the solution (10) becomes $\bar{T} = q/4\pi\kappa r$ which decays to zero at an infinite radial distance from the source. A variety of more practical situations can be deduced from (7) and (8) by integration, see section 7.3.

7.2. Single Continuous Line Source

[42] The temperature rise due to a finite line source supplying heat (per unit length) at a constant rate, $q_L\rho c$, may be obtained using the basic result derived in (10) for a continuous, constant point source. The solution is obtained by distributing these sources along the z axis from $z = a$ to $z = b$ and then integrating. The temperature rise, $\bar{T}_L$, at the point P with cylindrical coordinates R, z is then given by

$$\bar{T}_L = \frac{q}{4\pi\kappa} \int_a^b dz' \frac{erfc\left(\sqrt{\dfrac{R^2+(z-z')^2}{4\kappa t}}\right)}{\sqrt{R^2+(z-z')^2}} \tag{12}$$

Where $\sqrt{R^2+(z-z')^2}$ is the radial distance from one of the point sources to the point P. The integral in (12) cannot be evaluated explicitly but the numerical integration is very straightforward.

[43] For an infinitely long line source the integral in (12) can be performed explicitly giving

$$\bar{T}_{L\infty} = \frac{-q_L}{4\pi\kappa} Ei\left(-\frac{R^2}{4\kappa t}\right) \tag{13}$$

where $Ei(x)$ is the exponential integral defined by

$$-Ei(-x) = \int_x^\infty \frac{e^{-s}}{s} ds \equiv \left(E_1(x) = \int_1^\infty \frac{e^{-xt}}{t} dt, \quad x > 0\right) \tag{14}$$

where the term in brackets is related to Ei(-x) by analytic continuation.

[44] The same result (13) can also be obtained by integrating (8) from time = 0 to time = t for a constant rate of heating.

[45] As $t \to \infty$, the temperature $\bar{T}_{L\infty}$ behaves like ln (t) and hence tends to infinity; physically this means that the heat cannot get away from the source quickly enough. The infinite line source is a very useful result that can be used to approximate the temperature due to a stack of waste containers at small t and at a point near to the center of the stack. Further away from the stack, i.e., at very large distances, the point source result is a useful approximation to the temperature. As well as serving to validate the code, these results may be used to reduce the size of the mesh or reduce the computational effort.

[46] The GRANITE code has been tested against the solutions obtained in (12) and (13) for finite and infinite line sources with constant heat output. This was achieved by creating a cylindrical waste region 75 m long with a radius of 0.25 m in the GRANITE runs. This region contained 5 stacks of waste packages with the stacks separated by 2 m backfill spacers. The mesh points in this region were given a heat output of 10 kW per cubic meter. The waste grid points and surrounding grid points were all given the same thermophysical properties (see Table 1) and the ambient temperature was set to zero. The mesh point spacing was 0.03 m and the time step was 864 s. The temperature was determined at a number of points along a radius extending out from the midpoint of the waste stack ($z = 0$) for 3 different times: t = 100, 500, and 1000 days. For the line source calculations the heat output per unit length was chosen to

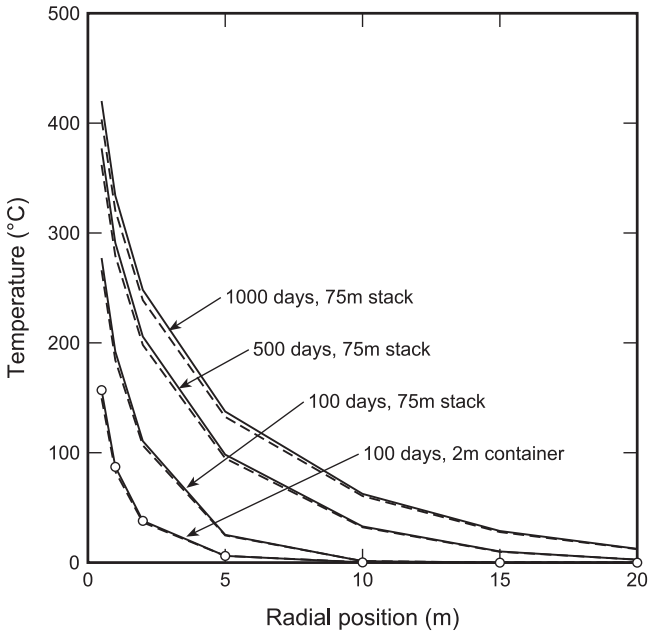

Figure 5. Comparison of GRANITE outputs (broken lines) for a 75 m stack (see text) with infinite line sources (continuous lines without symbols) and, for a single 2 m container, with a finite line source (continuous line with symbols). Ambient temperature was taken as 0°C in all cases.

match that used in the GRANITE calculations. For a cylindrical waste region, if H is the heat output per unit volume, then the heat output per unit length, q_L, = $Ha^2\pi$, where a is the radius of the cylinder. For the infinite line source calculations the $E_1(x)$ function was calculated using an algorithm given by *Press et al.* [1996], which employs a continued fraction representation for x > 1 and the series expansion for $0 < x < 1$ [*Abramowitz and Stegun*, 1970]. For the finite line source calculations a 7-point Gauss-Legendre method was used to numerically evaluate the integral. The complementary error function was calculated using an algorithm by *Press et al.* [1996]. As an additional test of the code, a GRANITE calculation was performed using a cylindrical waste region with a height of 2 m for the same radius of 0.25 m. These results were compared with the finite line source only. The calculated temperature is plotted against radial distance for the 2 line source models and GRANITE in Figure 5. The comparison for the long waste cylinder agrees well with the results of both line source models for the three values of elapsed time. The agreement diminishes slightly at 1000 days and can be expected to become worse at longer time periods since, as noted earlier, heat cannot escape quickly enough from the infinite line source. The agreement is also excellent between the finite line source and the small cylindrical waste region in the GRANITE simulation. This result can be exploited to reduce the size of the grid in the FD calculations.

7.3. Cylindrical Heat Source With Exponential Decay

[47] A model, quite closely related to the situation we are studying, can be constructed by taking a distribution of finite line sources, arranging them to form a solid cylinder and taking the heat supply to be an exponentially decaying function of time. This model has been studied in some detail by *Hodgkinson* [1977]. In this model, the heat source is a cylindrical radioactive waste region with a half-life, $t_{1/2}$, characterized by a decay constant, λ. The source term is thus given by $S = q_0 \exp(-\lambda t)$, where q_0 is the initial rate of heating per unit volume. This single container of waste is now taken to be surrounded by an infinite volume of rock which it is assumed has the same constant thermal properties as the waste, i.e., the same density, thermal conductivity and specific heat (see Table 1). *Hodgkinson* [1977] has shown that a semi-analytical solution can be obtained for this particular boundary value problem. The solution for the temperature rise is

$$\bar{T}(R,z,t) = \frac{q_0 e^{-\lambda t}}{4\rho c\kappa} \int_0^t d\mu \, \frac{e^{-\lambda\mu}}{\mu} \left\{ erf\left(\frac{z+b}{2\sqrt{\kappa\mu}}\right) - erf\left(\frac{z-b}{2\sqrt{\kappa\mu}}\right) \right\} \int_0^r R'\, dR'\, I_0\left(\frac{RR'}{2\kappa\mu}\right) \cdot \exp\left\{\frac{-(R^2+R'^2)}{4\kappa\mu}\right\} \tag{15}$$

where b is the cylinder half-length, r is the cylinder radius, I_0 is a modified Bessel function, while R and z are the radial and axial coordinates respectively. By defining r as the unit of length and r^2/κ as a convenient unit of time, the above expression can be written in terms of dimensionless quantities,

$$V(\sigma,\varepsilon,\tau) = \frac{e^{-\lambda\tau}}{4} \int_0^\tau d\mu' \, \frac{e^{-\lambda\mu'}}{\mu'} \left\{ erf\left(\frac{\varepsilon+\beta}{2\sqrt{\mu'}}\right) - erf\left(\frac{\varepsilon-\beta}{2\sqrt{\mu'}}\right) \right\} \cdot \int_0^1 \sigma'\, d\sigma'\, I_0\left(\frac{\sigma\sigma'}{2\mu'}\right) \exp\left\{\frac{-(\sigma^2+\sigma'^2)}{4\mu'}\right\} \tag{16}$$

where the various dimensionless terms have been defined as follows:

$$\sigma = R/r, \quad \varepsilon = z/r, \beta = b/r, \quad \tau = \kappa t/r^2, \quad \mu' = \kappa\mu/r^2,$$

$$\lambda = \lambda r^2/\kappa, \quad \text{and} \quad V = \bar{T}\kappa\rho c/(q_0 r^2).$$

[48] The expression in (16) simplifies in two special cases: case (i) when $\sigma = 0$, $\varepsilon = 0$ and case (ii) when $\sigma = 1$ and $\varepsilon = 0$, that is on the z axis and rock/waste interface respectively. In both

Table 1. Values of the Parameters Used in the Validation of the GRANITE Code Against Line Sources and the Case (Cylindrical Array of Line Sources With Exponentially Decaying Heat Source)

Property	K, $Jm^{-1}s^{-1}K^{-1}$	ρ, kg m^{-3}	c, J kg^{-1} K^{-1}	H, kW m^{-3}	q_0, kW m^{-3}	$t_{1/2}$, yr
Value	2.51	2600	879	10	1	30

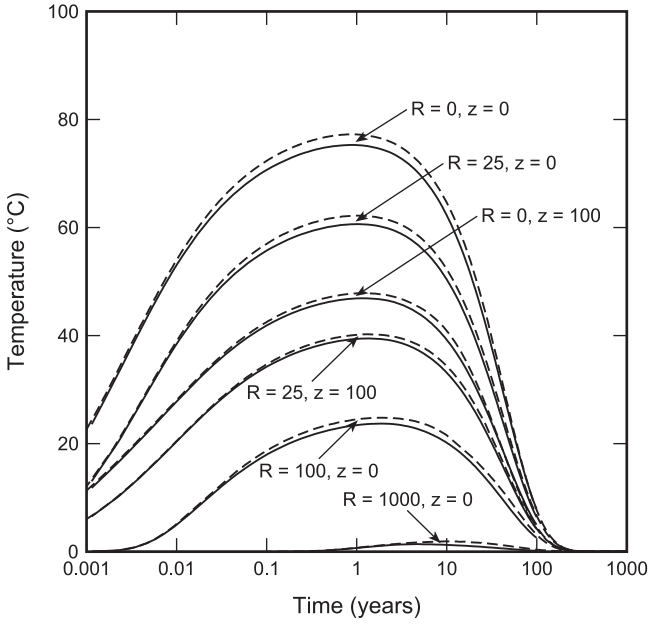

Figure 6. Comparison of GRANITE output (continuous lines) with numerical solutions to the problem considered by *Hodgkinson* [1977] (broken lines) for different axial and radial positions. Ambient temperature taken as 0°C.

cases the radial integral may be evaluated analytically leaving a much simpler one dimensional integral to be determined by numerical quadrature. For these cases, *Hodgkinson* [1977] has derived the following expressions for the temperature rise:

$$V(0,0,\tau) = e^{-\lambda\tau} \int_0^\tau d\mu'\, e^{-\lambda\mu'} erf\left(\beta/2\sqrt{\mu'}\right) \cdot \{1 - \exp(-1/4\mu')\} \quad (17)$$

$$V(1,0,\tau) = \frac{e^{-\lambda\tau}}{2} \int_0^\tau d\mu'\, e^{-\lambda\mu'} erf\left(\beta/2\sqrt{\mu'}\right) \cdot \{1 - \exp(-1/2\mu')I_0(1/2\mu')\} \quad (18)$$

[49] The GRANITE code was validated against the above model. The parameters for the model are given in Table 1. For these calculations a mesh spacing in the radial direction of 0.015 m was employed together with a time step of 1800 s. Temperatures were calculated at various times (spanning 6 decades on a log scale) at four different points located along a radial line extending out from the center of the waste stack (R = 0 cm, 25 cm, 100 cm, and 1000 cm).

[50] For the theoretical models, two of the points chosen coincide with the special cases mentioned above ($z = R$ = 0 cm, and z = 0, R = 25 cm). In these cases, the temperature was obtained by numerically integrating (17) and (18) using a 7 point Gauss-Legendre method with 1000 intervals for the time integrals. For the remaining two points of interest the temperature was evaluated from (16) using the same quadrature method as before, but now applied to both integrals. The modified Bessel function, $I_0(x)$ was calculated using an algorithm given by *Press et al.* [1996], based on polynomial approximations given by *Abramowitz and Stegun* [1970]. Figure 6 shows the variation of the temperature rise with time The continuous lines represent data obtained from the semi-analytical solutions (16–18) above, while broken lines represent the data obtained from the GRANITE code. There is good agreement between the two sets of results across the range of spatial points studied. However, it should be noted that the GRANITE results are systematically higher than those predicted by equations (16)–(18) but the differences are never greater than 5%. These small discrepancies can probably be attributed to the treatment of the rock-waste boundary.

[51] In conclusion it can be seen that the instantaneous point source model is a very useful building block from which a number of useful models can be created (line source with constant heat output and cylinder of line sources with exponentially decaying heat output). These models have been used to demonstrate that the GRANITE code can produce sensible results. While these models can also be useful for giving some physical insight into the conductive flow of heat, in more complicated situations they must be replaced by the FD method used in GRANITE for cases in which the thermal properties are temperature and time dependent, and for more complex source terms.

8. Constraints and Uncertainties

[52] There are a number of constraints on the model that fall into three categories. First, there are assumptions about the physical model that must be made to reduce the complexity to manageable levels or are so self-evident that it would be absurd not to make them. Secondly, there are computational constraints inherent in the approach and thirdly, there are limitations to the quality and availability of data used to generate the numerical solutions.

8.1. Physical Assumptions

8.1.1. Axisymmetry

[53] The concept of deep borehole disposal (DBD/VDD) is based on drill holes with a circular cross-section and consequently all the key components such as the casing and waste containers are likewise circular. In principle therefore the model is axisymmetric but, in practice, there could be departures from this. Individual containers might not be exactly centered with respect to the casing, which itself might depart locally from centricity with the borehole wall, which in turn could be slightly elliptical due to anisotropic stress breakout. However, such departures would generally be small and tend to average out. More difficult to guarantee are the petrologic homogeneity and uniformity of physical properties of the host rock implicit in an axisymmetrical model. While rocks such as granite can be surprisingly homogeneous on the scale of tens of meters they can also vary considerably and anisotropy is not uncommon, especially where a fabric is present. Given that (1) DBD would aim for as uniform host rocks as possible, (2) that key thermal properties are unlikely to vary significantly without major chemical and mineralogical changes in the rock and (3) that any anisotropy would be site-specific and could only be evaluated after exploratory drilling, a generic model must assume axisymmetry. Such an assumption enables

modeling of the heat transfer in only two spatial dimensions greatly simplifying the problem.

8.1.2. Heat Transfer Mechanisms

[54] For the purposes of the modeling it is assumed that heat transfer is predominantly by conduction. The possibility of significant heat transfer by convection may arise in specific parts of the DBD system where liquids or partly liquid materials are present, albeit on a transient basis. These are discussed further in the appropriate places (see section 10) and it is concluded that, with the possible exception of the borehole fluid above the waste packages during emplacement, the effects are likely to be so small they can be ignored. The possibility of heat transfer by radiation does not really arise as only in the HTVDD version are temperatures likely to occur that might approach those where radiation becomes significant. In such cases there would be no gaseous or liquid volumes transparent to thermal radiation in the system.

8.1.3. Uniformity of Heat Source

[55] The model can accommodate different thermal loadings of the waste containers but assumes the distribution of heat-generating matter within an individual container is uniform. For vitrified HLW, such as used in LTVDD-1, this is to be expected and any departure from it would be all but impossible to confirm and measure. For spent fuel rods embedded in a non-heat-generating matrix, as in LTVDD-2 or HTVDD, this is clearly not true on a small scale. However, as the packing density approaches the theoretical maximum, it becomes a very good first approximation on the scale of a container and, given that the exact positions of individual fuel pins within the container can not be ascertained precisely once the container is filled and sealed, a uniform distribution of the heat source is a necessary and reasonable assumption.

8.1.4. Thermal Contact

[56] It is assumed that all the components of the physical model are in perfect thermal contact with each other throughout the heating and cooling cycle. Since voids anywhere between the containers and host rock will be filled with aqueous fluid (or partly melted HDSM in the case of LTVDD-2) this will be true outside the container. However, inside containers filled with glass (vitrified HLW in LTVDD-1 and borosilicate glass infill in one version of LTVDD-2) it is conceivable that differential thermal expansion of the glass and metal container could result in small gaps between parts of the container wall and its contents. We have not analyzed the effects of this in any detail but it seems most unlikely that the overall heat transfer would be reduced significantly.

8.2. Computational Constraints

8.2.1. Boundary Condition

[57] It is obvious that at some distance from the borehole the thermal effects of the disposal will be negligible and the temperature of the rock will equal the ambient value at the depth in question. This can be used to set the boundary condition for the model, although the actual distance will increase with time, i.e., the duration of the solution. By starting with very large values (hundreds of meters) and experimenting with ever decreasing distances we ascertained that, for solutions less than 10,000 days, the position of the ambient temperature boundary does not significantly affect the modeled temperature distributions until it is less than 10 m from the borehole wall. Consequently the boundary has been set at 50 m from the axis for most of the modeling.

8.2.2. Mesh Dimensions

[58] The overall size of the mesh (section 6.1) is controlled by the geometry of the disposal being modeled and the position of the ambient temperature boundary but the number of nodes in the mesh and their spacing can be varied. For large intervals between the mesh lines the results become a function of the spacing, i.e., errors are introduced, and for very small intervals the number of nodes becomes such that the demands on computing time and memory are excessive. Consequently, considerable attention has to be given to the design of the mesh with the nodes more closely spaced in the areas of greatest interest, i.e., around the containers and borehole wall, and more widely spaced elsewhere, e.g., in the more distal regions of the wall rock, although too rapid changes in spacing have to be avoided. The spacing of the mesh points is always such that further increasing the point density would not significantly improve the temperature solution. It is also assumed that any expansion or contraction does not affect the thermal properties allocated to the mesh points (see section 8.3.1).

8.2.3. Time Increments

[59] It is well known that the choice of time steps in FD modeling can be critical. For the implicit method used (5) too large a step will not result in instability of the equations but the accuracy of the solution will deteriorate significantly. If the time step is too small the computation and the time required to generate a solution become un-necessarily large. The use of variable time step integration schemes could be helpful in this respect although in this work we have used a simpler, more pragmatic approach which involves increasing the time step once the peak cooling has been achieved (which then remains constant for the remainder of the simulation). Again we have ascertained the suitable range of time increments by trial and error and for most of the modeling have used a time step of the order of 1 h.

[60] The typical computational time for a 1000 year simulation is about two hours.

8.2.4. Duration

[61] The time over which heat output from the waste affects the environment around a DBD can be tens (if not hundreds) of millenia. However, the roughly exponential nature of the decay means that the period over which the thermal effects are really significant is rarely more than a hundred years and often substantially less. Although none of the applications for which we have used GRANITE to date has required modeling for over 200 years, longer runs would require increases in the time step after this interval if excessive computing demands are to be avoided.

8.3. Data Limitations

[62] The main physical properties required for modeling are density (ρ), specific heat capacity (c) and thermal conductivity (K) but the range of possible materials for which values are needed is considerable. Among these are UO_2, borosilicate glass and vitrified HLW (waste forms); stainless steel, copper, titanium, alumina, zirconia (container materials); mild steel (casing); cementitious grouts, Pb, Pb-Sn-Bi alloy HDSM, granitic backfill, water, brines (fillings); and granite and related rock types (host rocks). A further

complication arises from the fact that the properties of many of these materials, especially steel, cements, backfill and rock, will vary with their composition. In such cases we have had to opt for values for a composition we regard as a likely candidate for the application in question, e.g., stainless steel 316L for containers. While every effort has been made to get the best values available for each material, some of the data are elderly and/or of questionable reliability and where different values exist for the same parameter some exercise of judgment has been necessary.

8.3.1. Temperature Dependence of Properties

[63] All three main properties vary with temperature but unfortunately the dependence is not always known with certainty (and sometimes not at all) for many of the materials concerned. This is especially so over the full temperature range of interest for the modeling (0°C to 500°C and, for HTVDD, occasionally to >1200°C).

[64] GRANITE can calculate the temperature dependence of density provided the coefficient of thermal expansion is known for the material. However, this might not yield true values given the pressure at the bottom of the borehole and it introduces the possibility of expansion moving material interfaces across mesh nodes or the mesh having to be iteratively expanded and contracted. All of this would greatly increase complexity and computing time and is unlikely to be justified, especially if the density decreases with temperature do not lead to significant changes in the outcome of the modeling (section 9.1).

[65] Data are available for the temperature dependence of specific heat capacity and thermal conductivity of some of the above materials, including granite, borosilicate glass, UO_2 (SNF) and steel, but not for all. Where reliable data are available, the thermal dependencies of these parameters are built in to the code. Undoubtedly, the most crucial of these are the thermal conductivities and specific heat capacities of the host rocks and for these we use the values and temperature dependencies calculated from the equations given by *Vosteen and Schellschmidt* [2003]. Where there is uncertainty about values or their temperature dependence we have attempted to ascertain the effects of these on the outcome of the modeling by evaluating solutions using realistic limiting cases (sections 9.2 and 9.3).

8.3.2. Backfill

[66] An important material in the physical model is backfill consisting of a concentrated aqueous slurry of crushed host rock (granite). No values have been determined for the thermal properties of this material but it seems intuitively reasonable to use values intermediate between those of water and those of granite. Although we have elected to use a 3:1 granite:water weighted average for each property, we appreciate that the relationships may not be linear and that for a property like conductivity there may be a threshold concentration above which it changes dramatically. A further complication may arise from the physical state of the backfill (see section 9.4). Again we have evaluated the effect of this uncertainty on the modeling results (section 9.4).

8.3.3. Borehole Fluid

[67] A range of water-based fluids ('muds') is likely to be used during the drilling of the borehole and emplacement of the waste packages. By the time deployment of the packages is complete, the remains of these will have become mixed with the intrarock fluids, which, under the conditions envisaged for DBD, are likely to be fairly concentrated NaCl, $CaCl_2$ brines [*Moller et al.*, 1997]. Since the precise nature of the aqueous fluid in the hole is site-specific and can only be known once an exploratory or pilot hole is drilled, it is assumed for the purposes of generic modeling that the fluid has the thermal properties of pure water. However, an attempt to quantify possible errors on the modeling arising from this assumption is made in 9.5 using a surrogate brine solution.

8.3.4. Decay of Heat Source

[68] Heat sources used in the modeling are actual examples of vitrified HLW and spent LWR fuel. Heat outputs from these and their decay are calculated using FISPIN [*Burstall*, 1979]. The forms in which the data are available to us are tables of outputs (in kW per canister and kW per tHMi (ton of initial heavy metal) respectively) at given times after removal from the reactor. A log heat versus log time plot is constructed from these values (Figure 4) and used, with linear interpolation between the data points, to model the time dependence of our heat sources. This gives a suitably close fit to the true decay curves (section 6.4).

8.3.5. Latent Heat

[69] In one version (HTVDD) the heat from the waste partially melts the rock necessitating that some of the thermal energy from the waste is used to overcome the latent heat of melting. As a result, less energy would reach any point in the host rock than by conduction through the solid state alone thus reducing the maximum temperatures attained and increasing the times taken to reach them. It should however be noted that this energy is released again when the melt eventually cools and recrystallizes.

[70] Latent heats of melting are poorly documented for rocks but are generally thought to fall in the range 271,000 to 419,000 J kg^{-1} [*McBirney*, 1984] and increase with depth by ~1% per km [*Yoder*, 1976]. For evaluation of latent heat effects on the modeling a value of 300,000 J kg^{-1} is used for granite. In reality, under the conditions likely for HTVDD, granite melts over a temperature range from ~700°C to ~1150°C [*Attrill and Gibb*, 2003a; *Whitney*, 1975].

[71] Unfortunately, not enough is known about how latent heat is proportioned between the different mineral phases in granite and over their melting intervals to model the effects accurately. Knowing the relationship between temperature and the degree of melting should enable a good first approximation to be calculated for the consumption of latent heat during partial melting but this depends strongly on the amount of water present (Figure 7). The water contents of the backfill (or the compacted sediment derived from it) and the host rock beyond the borehole wall are unknown but are likely to be very different. The water content of the granite would probably be little more than the H_2O^+ value of the rock, i.e., <1%, whereas that of the backfill could be well over 10% (hence giving rise to saturated melting) [*Attrill and Gibb*, 2003a]. Under these circumstances the significance of the latent heat of granite melting in the model for HTVDD is best evaluated using limiting cases (section 9.6).

9. Significance of Data Limitations

9.1. Density

[72] To evaluate the importance of temperature dependence and any data uncertainties for this (and other) properties a

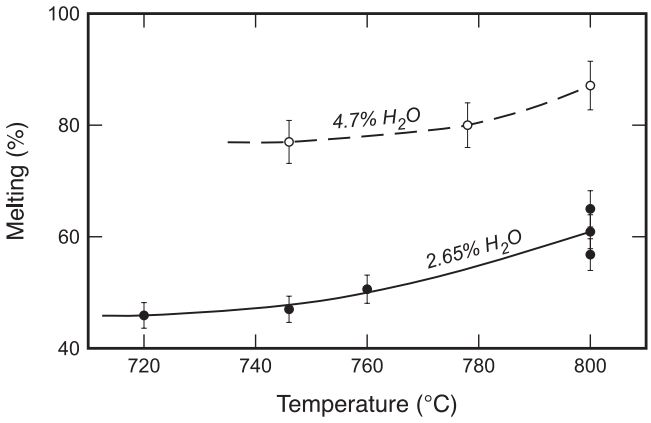

Figure 7. Relationship between amount of melting and temperature for granite E93/7 at two levels of total water content [after *Attrill and Gibb*, 2003a].

control solution was generated for a simple case of LTVDD-2 using a single stainless steel container (1.5 m × 0.315 m radius and wall thickness 0.05 m) filled with 2 year old SNF. For the 500 day solution a time step of 1800 s was used and all material properties were assumed to be independent of temperature.

[73] The materials for which a decrease in density with increasing temperature is most likely to affect the outcome are stainless steel (with the highest coefficient of thermal expansion) and the host rock (which has the greatest total volume). Re-running the control solution with temperature dependent density for the stainless steel container resulted in decreases in the temperature at key points mid-way up the waste package on the borehole wall and 0.4 m out into the host rock of less than 0.005 %. The thermal expansion of granite, and hence the decrease in density with temperature, is substantially less than for steel, and no detectable effects on the temperature distributions were found. Given the other uncertainties inherent in the model and the data used, such small effects cannot justify the extra computing demands and, consequently, for all materials used in the modeling the temperature dependence of density is ignored.

9.2. Specific Heat Capacity

[74] Apart from the host rock (for which temperature dependence of specific heat is always used), the materials for which this property is most likely to affect the solution are the waste itself (SNF) and the stainless steel container. Re-running the control solution with the specific heat capacity dependent on temperature for either of these materials resulted in temperature decreases at the key points on the borehole wall and 0.4 m out into the host rock of less than 0.03 %. Consequently, the temperature dependence of specific heat capacity for all materials except the host rock can safely be ignored in the modeling.

9.3. Thermal Conductivity

[75] Again with the exception of the host granite (for which temperature dependence of thermal conductivity is always used) the materials for which temperature dependence of thermal conductivity is most likely to affect the results are the SNF and the steel. Re-running the control solution with the thermal conductivity of SNF temperature dependent increased the 500 day temperatures on the outside of the container, at the borehole wall and 0.4 m out into the granite by 4.0 %, 3.8% and 3.1% respectively. With the thermal conductivity of the stainless steel dependent on temperature the same points decreased in temperature by 4.7 %, 4.6% and 4.0 %. Clearly such effects are significant and, while they act in the opposite sense and tend to cancel each other out, they must be taken into account in the modeling. Consequently, temperature dependent thermal conductivity is used in the modeling for all materials for which we have meaningful data.

9.4. Backfill

[76] In running the control solution a 3:1 granite to water backfill was used with the thermal properties proportioned 3:1 between those of granite and water. In addition to the uncertainty of such a linear relationship, especially for thermal conductivity, there must be questions about the physical condition of the backfill in any part of the VDD/DBD system. Whatever the ratio of the rock:water mix introduced into the borehole, redistribution of the suspended particles is bound to occur. For example, in the annulus between the waste packages and the borehole wall gravity settling will result in much higher rock:water ratio that could easily approach the maximum possible packing density. For a suspension of irregularly shaped particles of variable size it is possible, indeed probable, that this annulus would become filled with a very dense sediment of granitic composition with only a small amount of fluid in the interstices. [Such sedimentation would also have consequences for the possibility of thermal convection occurring in the backfill (see section 10).] In such cases our estimate of properties 75% of the way between water and granite are likely to be an underestimate.

[77] Consequently, two limiting cases were run; the first assigning the thermal conductivity of solid granite to the backfill and the second using the thermal conductivity of water. For a point mid-way up the waste package the temperature on the borehole wall increased by 0.82% in the first case and decreased by 4.8% in the second. In the granite 0.4 m out from the borehole the temperature increased by 0.75% in the first case and decreased by 4.1% in the second. Realistically, the thermal conductivity of the backfill is likely to be somewhere between that of granite and that calculated for our 3:1 mixture so any error is likely to be smaller than 0.82%.

9.5. Borehole Fluid

[78] It is conceivable that uncertainties in the thermal properties of the borehole fluid could give rise to significant errors in the modeling solutions. We have attempted to quantify this by running the control solution with the borehole fluid (both above the container stack and in the pore spaces of the backfill) having the (constant) thermal properties of, first, pure water and then 1 molal NaCl solution (both at 100°C). The latter is a simplified approximation to the NaCl - $CaCl_2$ brines found at depths of a few km in continental crustal rocks. The differences in thermal properties are small (around 1%) and, for the key points on the borehole wall and 0.4 m out into the host rock, temperature differences between the two solutions were less than 0.01%.

[79] A potentially larger error could arise from the unusual temperature dependence of the thermal conductivity of saline fluids. For example, the thermal conductivity of 4 molal NaCl solution rises from ~0.55 $Wm^{-1}K^{-1}$ at 0°C to ~0.68 $Wm^{-1}K^{-1}$ at 150°C then falls to ~0.51 $Wm^{-1}K^{-1}$ at 300°C. To evaluate the effects of such variations we ran the control solution with the thermal conductivity of the borehole fluid varying by 0.45 $Wm^{-1}K^{-1}$ and recorded changes in temperatures on the borehole wall and 0.4 m out into the host rock of less than 0.25%. Clearly, any errors arising from the smaller variations in thermal conductivity of the borehole fluid likely to arise in real DBD scenarios can reasonably be ignored.

9.6. Latent Heat

[80] There are two bounding cases that define the possible effects of latent heat on the temperature distribution in the host rock once partial melting of the granite begins in a HTVDD. The first assumes the latent heat of melting is all consumed at the solidus temperature (~700°C) and the second that none of it is consumed until the liquidus temperature, i.e., in the case of partial melting no latent heat is consumed. These two cases have been modeled [*Gibb et al.*, 2008b] for a HTVDD of 5 containers of 4 year old SNF. It was found that the largest difference in temperature between the two limiting cases (9%) occurs at the borehole wall soon after melting begins but this decreases rapidly with both time and distance into the wall rock. Although this difference is not trivial, it is transient. More significant is the fact that the maximum temperatures attained at the borehole wall and 0.4 m out into the wall rock are reduced by less than 1% because of latent heat. However, it is noteworthy that the delay in achieving maximum temperature at the borehole wall is almost 10%, although 0.4 m out it is less than 1%.

[81] Since most of the melting of the granite takes place over the first 100 – 150°C of the > 400°C melting interval [*Attrill and Gibb*, 2003a] the assumption that all of the latent heat is used at the solidus is likely to give the better approximation to reality. Also, this assumption yields the lower wall rock temperatures and so is conservative when used to predict the extent of the sarcophagus of melted and recrystallized rock in HTVDD.

10. Convection

[82] The introduction of heat sources into the borehole raises the possibility of thermal convection occurring in any fluids present. In theory this could take place within the borehole itself or in the saline brines present as intrarock fluids in the granite beyond the borehole wall, or in both.

10.1. Borehole

[83] Following the deployment of the waste packages, aqueous fluids could be present in the annulus between the containers and casing and, unless the casing is cemented in, in the irregular gaps between the casing and borehole wall. They would also be present in the borehole above the top of the stack of containers. Exactly where, and for how long, such fluids are present varies with the exact version of DBD/VDD involved.

[84] For LTVDD variants any spaces between the containers and wall rock are filled with materials (grouts or high-density support matrices) immediately after deployment of the containers. Aqueous fluids are expelled from these materials within a few weeks [*Gibb et al.*, 2008a, 2008b] and there is therefore very limited scope for any convection within the borehole, except possibly temporarily in the borehole fluid some meters above the top container before the next batch is deployed (see below).

[85] It is in the case of HTVDD that there is most likely to be an opportunity for convection within the borehole. Following emplacement of the waste packages, the gaps between the containers and the borehole wall are filled with a concentrated aqueous suspension (slurry) of crushed host rock (granite) to a height of several meters above the containers. Settling of the solid particles within this suspension (section 9.4) will be quite rapid and give rise to a density compacted sediment in the annulus between the containers and borehole wall and for some distance above the topmost container. In the case of single or batch emplacement this sediment may only extend upwards for one or two meters but after the last container is emplaced and the borehole backfilled it would be for several hundred meters. The compaction and water content of these sediments will have a significant bearing on the potential for convection (of the whole sediment or the fluid phase within it) in the annulus around the containers and immediately above them. Particle-free or particle-poor fluids would normally only exist in the column above the waste packages for relatively short periods (days) between emplacements but we have to consider the possibility of delays during which there might be a substantial column of aqueous fluid above the thin sediment layer on top of the last container to have been emplaced. In such cases the problem comes down to heat transfer through the sediment layer and into a fluid column with the potential for upwards transfer of heat through coupled conduction and convection. Although a transient phenomenon, this is an aspect of the wider problem that we are continuing to investigate as it could lead to a significant loss of heat from the disposal. Should further studies indicate that significant convection might occur in the backfill we would also investigate the possibilities of similar phenomena in the setting cement grouts used in LTVDD-1 and in the fluid component of the HDSM in LTVDD-2 prior to melting of the alloy.

[86] Once the granite in the backfill around the containers and the wall rock itself begin to melt at around 700°C, the supercritical aqueous fluid would be expelled upwards into cooler regions of the borehole by the sinking of the denser silicate melt. It has been calculated [*Gibb et al.*, 2008b] that this would take between four months and a year after emplacement. Given the extremely high viscosities of granitic liquids around 800°C (~10^5 Pa s) there is little likelihood of significant convection in the silicate melt. The key issue, therefore, is whether thermal convection might take place in the annulus of backfill during this interval and whether it might significantly affect the heat distribution within the model.

[87] A quantitative solution to this problem is extremely complex and is beyond the scope of this paper. However, the possibility of convective uprise, either of the backfill or within its fluid phase, may justify the precaution of inserting an impermeable spacer a short distance above the top of each container (or stack of containers) to prevent significant

upwards heat loss (see above). It certainly warrants generating 'limiting case' solutions for the conductive heat transfer model in which temperature gradients within the backfill annulus are averaged out to simulate thermal homogenization as a result of convection. If significant homogenization occurred in the backfill annulus during the pre-melting stage of a HTVDD it could be extremely helpful in reducing the effects of temperature variations along the length of the stack [*Gibb et al.*, 2008b].

10.2. Intrarock Fluids

[88] The unavoidable presence, however small, of aqueous fluids within voids and fractures in the granitic host rock could give rise to large scale convective circulation provided both the heat source and the bulk hydraulic conductivity of the rock are large enough. The emplacement of containers of radioactive wastes producing enough heat to generate partial melting of the granite around the borehole, as in HTVDD, would seem capable of supplying more than enough heat for convection. On the other hand, the low vertical hydraulic conductivities ($\sim 10^{-11}$ m s^{-1} [*Toro*, 1990; *Gibb*, 2000; *Stober and Bucher*, 2004]) commonly prevailing in likely host rocks for DBD would severely restrict the extent of any convection. Hydraulic conductivities recorded from continental crustal rocks at depths greater than 3 km generally range from 10^{-7} to 10^{-14} and in regions with the higher values there would be potential for considerable convection to occur. However, such regions are unlikely to be chosen for DBD of radioactive wastes.

[89] Convective transport in the present context is important when considered as a possible mechanism for the transportation of radioactive particles from the intrarock fluids into which they could be leached following containment failure to the biosphere. Convection currents arise naturally from buoyancy effects. To determine the typical trajectory of a particle in the presence of natural convective currents requires a numerical solution of the equations of continuum fluid mechanics. Typically such a calculation would be conducted using a commercial computational fluid dynamics software package. However, it is instructive to obtain an analytical solution for a simplified version of the full problem employing some judiciously chosen approximations.

[90] Heat transfer occurs in reality by both conduction and convection and ideally requires a coupled solution of the continuum field equations. However, given the low bulk hydraulic conductivities of the host rock, heat transfer by conduction is orders of magnitude faster than by convection, allowing solution as separate linear problems using the heat provided by conduction as the heat source driving convection currents [*Hodgkinson*, 1979].

[91] On a large enough scale (km), and as a first approximation, the problem of a HTVDD of, say, two 0.63 m diameter $\times$ 3.75 m long containers of 4 year old spent fuel can be treated as a point heat source in an infinite medium. If we ignore transient heating effects, instead seeking a steady state solution of the problem, the temperature rise due to a point source of heat follows by taking the limit t $\rightarrow \infty$ of equation (10),

$$\bar{T} = T - T_0 = \frac{q}{4\pi\kappa r}, \tag{19}$$

where T_0 is the initial (ambient) temperature.

[92] For flow through a porous medium in a gravitational field, in which a pressure gradient drives the flow, the velocity, $\boldsymbol{u}$, of a fluid element is given by the modified version of Darcy's law,

$$\frac{\eta}{k}\mathbf{u} = -\nabla(p_0 + p) + \rho_0 g\beta\,\mathbf{k}(T - T_0) - \rho_0 g\mathbf{k} \tag{20}$$

where η is the dynamic (shear) viscosity, p is the scalar pressure, p_0 is the hydrostatic pressure, k is the permeability (note that in some textbooks this quantity is referred to as the specific permeability, since it is a property of the porous material alone), β is the coefficient of volume expansion, $\beta = -\rho^{-1}(\partial\rho/\partial T)_p$, g is the acceleration due to gravity, ρ_0 is the fluid density at the reference temperature, T_0, while $\mathbf{k}$ is a unit vector directed along the z-coordinate axis. Equation (20) has been derived by adding a term $\rho g\boldsymbol{k}$ to Darcy's law, replacing the density, ρ, by its Taylor expansion about T_0, (truncated after the first derivative). Note that we allow only temperature variations of the density in the buoyancy term (Boussinesq approximation).

[93] Equation (20) together with equation (19) must now be solved for $\mathbf{u}$. Since there are two unknowns, an additional equation must be supplied. For an incompressible fluid, mass conservation implies

$$\nabla \cdot \mathbf{u} = 0 \tag{21}$$

[94] A closed solution involves solving first for the pressure and then eliminating this as an independent variable before solving for $\mathbf{u}$.

[95] To achieve step 1 we first remove the hydrostatic part of the pressure from equation (20), {i.e., set $T = T_0$, $\boldsymbol{u} = 0$, $p_0 = -\rho_0 gz$}, take the divergence and change to spherical polar coordinates (r, θ, ϕ), to give

$$\frac{\partial}{\partial r}\left(r^2\frac{\partial p}{\partial r}\right) + \frac{1}{\sin\theta}\frac{\partial}{\partial\theta}\left(\sin\theta\frac{\partial p}{\partial\theta}\right) = -A\cos\theta, \tag{22}$$

where A is a constant given by $A = \frac{\rho_0 g\beta q}{4\pi\kappa}$. Assuming that the pressure has no radial dependence and that it must remain finite, (22) has the simple solution,

$$p = \frac{1}{2}A\cos\theta \tag{23}$$

[96] When (23) is substituted into (20) we may solve for the velocity of a fluid element (ignoring the hydrostatic term). This gives

$$\boldsymbol{u} = \frac{C}{r}\left(\frac{1}{2}\sin\theta\,\hat{\boldsymbol{\theta}} + \boldsymbol{k}\right) \tag{24}$$

where C is now a new constant related to the constant A by $C = (k/\eta)A$ and $\hat{\boldsymbol{\theta}}$ is a unit vector in the direction of increasing polar angle, θ. We note that C is also closely related to the Rayleigh number.

[97] It proves convenient for the present purposes to change to a cylindrical polar coordinate system. Upon performing this

coordinate transformation we obtain the velocities of the fluid element in the radial and axial directions, respectively,

$$\frac{dR}{dt} = \frac{C}{2} zR\left(R^2 + z^2\right)^{-3/2}, \tag{25}$$

$$\frac{dz}{dt} = \frac{C}{2}\left(R^2 + z^2\right)^{-3/2}\left(R^2 + 2z^2\right) \tag{26}$$

[98] This coupled pair of equations may be integrated to yield the trajectory of the moving fluid element,

$$R = a\cosh\lambda \tag{27}$$

$$z = a\cosh\lambda\sinh\lambda \tag{28}$$

where a is the radial position of a fluid particle when $z = 0$ and λ is a parameter related to the time, t, that can be obtained as the solution of

$$t = \frac{a^2}{C}\left[\frac{1}{2}\sinh\lambda\cosh^3\lambda + \frac{3}{4}\sinh\lambda\cosh\lambda + \frac{3}{4}\lambda\right]. \tag{29}$$

[99] The parameter C may be simplified by introduction of the hydraulic conductivity, $\psi = g\rho_0 k/\eta$, giving $C = \frac{\psi\beta q}{4\pi\kappa}$. We note that the hydraulic conductivity is a composite property of the fluid and the porous material through which it is flowing.

[100] To determine how far an element of fluid will travel in the vertical direction for a given starting point along the radial axis, we need to determine a value for C. For the purpose of this calculation we have taken a value of $\beta = 0.00075\ \mathrm{K}^{-1}$ for pure water at 100°C and 1 atm pressure [*Einsenberg and Kauzmann*, 1969]. For the hydraulic conductivity we have used a value appropriate to granite at a depth of several kilometers. This value is $\psi = 10^{-11}\ \mathrm{ms}^{-1}$. The thermal diffusivity has been calculated from values of the thermal conductivity, density and specific heat capacity of granite at 100°C. These values are respectively, 2.106 W $\mathrm{m}^{-1}\ \mathrm{K}^{-1}$, 2630 kg m^{-3}, and 874.0 J $\mathrm{kg}^{-1}\ \mathrm{K}^{-1}$, giving a thermal diffusivity, $\kappa = 9.162 \times 10^{-7}\ \mathrm{m}^2\ \mathrm{s}^{-1}$. The heat output from the contents of the two containers of 4 year old SNF (above) is 15.31 kW m^{-3}. If the internal volume of each container is 0.9416 m^3 this gives a total heat output of 28.83 kW for the 2 container stack. In terms of the q in (22), this gives $q = 1.254\ 10^{-2}\ \mathrm{K}\ \mathrm{m}^3\ \mathrm{s}^{-1}$. The constant, C, is then $C = 8.170 \times 10^{-12}\ \mathrm{m}^2\ \mathrm{s}^{-1}$.

[101] We have calculated the value of z (the total vertical displacement due to convection) for 3 different radial positions: a = 0.1 m, 1 m, and 10 m for a time of 250,000 years. Our calculations result in the following respective values for z: 11 m, 10 m and 3 m. These values represent a worst-case-scenario since in reality, the heat source is decaying and any thermally driven convection will eventually cease. It has been calculated [*Gibb et al.*, 2008b] that the elevated temperatures in the rock around such a HTVDD returns to within a few tens of °C of ambient in less than 300 years. Thus from the magnitudes of the values we obtained it is obvious that the effects of convection occurring in the intrarock fluids around even high-temperature DBD at these depths can be discounted.

11. Applications

[102] The importance of acquiring information on the distribution of temperature with time in and around borehole disposals was outlined in 3 and examples of specific applications of the model are summarized below. In two of these examples case studies involving the numerical outcomes from GRANITE are reported to illustrate how the model can be used to demonstrate how the HDSM works in LTVDD-2 and to calculate the size and shape of the recrystallized granite sarcophagus in HTVDD.

11.1. Performance of Materials

[103] All high-level wastes generate heat and in DBD the temperatures of all of the materials involved (waste form, container, borehole fillers, casing, rock, etc.) pass through a maximum sometime after disposal before cooling. These temperatures are increased relative to many other forms of storage and disposal by the thermal insulating effect of the host rock. In designing any DBD/VDD strategy it is necessary to ensure that the long-term performance of none of the materials is jeopardized by the maximum temperatures attained and for each scenario there is usually one temperature limiting component. For LTVDD-1 this is likely to be the high-temperature cementitious grout (similar to those used in geothermal energy wells) used to seal the vitrified HLW containers into the borehole whereas for HTVDD it will be the container itself. Examples of temperature/time distributions for various DBD cases were given by *Gibb et al.* [2008b], who showed that they can be kept within the necessary specifications by appropriate design of the disposal (particularly the size, number and thermal loading of the containers) based on predictive modeling.

11.2. HDSM

[104] A novel concept for the DBD of spent nuclear fuel rods [*Gibb et al.*, 2008a] involves the use of special high-density support matrices (HDSM) to overcome vertical stress loading problems and "solder" the containers into the borehole. These are Pb-based, low melting point alloys, deployed along with the waste packages as fine shot, that require to be melted by the heat from the waste in order to function properly. Prediction and control of this process necessitates knowledge of the distribution of temperature with time in the annulus between the waste packages and the borehole wall. To show how the model can be used to obtain this information and demonstrate that the HDSM will work, *Gibb et al.* [2008a] modeled the case of 10 stainless steel containers filled with 73% of 30 year old PWR fuel pins (45 GWd/t burn-up) with a Pb infill. These waste packages, which were deployed at 2 day intervals, have a specific gravity of 10.1 necessitating a HDSM with a specific gravity of ~9.7. This was provided by a $Pb_{70}Sn_{30}$ alloy with a solidus temperature of 183°C. The other parameters used in this model, which is case A of *Gibb et al.* [2008a], are given in Table 2.

[105] The results are shown in Figure 8 in which each curve relates to the temperature evolution in the HDSM at a

Table 2. Parameters Used in the Modeling of LTVDD-2 and HTVDD Case Studies

Parameter	LTVDD-2	HTVDD
Borehole diameter, m	0.8	0.8
Container diameter, m	0.63	0.63
Container height, m	3.75	1.5
Container wall, m	0.05	0.03
Waste type	PWR spent fuel	PWR spent fuel
Infill	Pb	Borosilicate glass
Waste thermal conductivity, W m^{-1} K^{-1}	12.52	4.33
Waste specific heat, J kg^{-1} K^{-1}	209.9	402.6
Waste density, kg m^{-3}	11070.3	8601.5

point adjacent to the container surface. Assuming an ambient temperature of 100°C at 4 km, the HDSM begins to melt at the mid point of the stack (curve 1) 17 days after the first deployment while at the bottom (curve 2) and top (3) of the stack initiation of melting takes 29 and 120 days respectively. The maximum temperature attained is 356°C at the mid point of the stack after 5.5 years and solidification begins at the top of the stack 49.5 years after deployment commenced. The solidification of the HDSM is complete (at the mid point of the stack) after about 125 years. Clearly the temperatures attained in and around the borehole, and the times taken to reach them, can be tailored to the requirements of the disposal by adjustment of the type and age of the spent fuel and other parameters, such as the fuel pin to infill ratio and the dimensions, spacing and emplacement rate of the containers. The results of the modeling demonstrate that the HDSM will remain at least partly molten until long after the deployment of containers is completed and the borehole sealed up. The benefits of this and other aspects of the function of the HDSM are discussed by *Gibb et al.* [2008a].

11.3. Design of HTVDD Strategies

[106] The objective of HTVDD is to generate an envelope of partially melted granite backfill and host rock around a stack of waste packages that, on cooling slowly as the heat output of the waste decays, will recrystallize to form a sarcophagus of solid granite and entomb the waste. At the same time it is important that the integrity of the waste containers themselves is not jeopardized before the granite sarcophagus has recrystallized. The thickness and extent of the sarcophagus is determined largely by the size and number of containers in the stack, and especially by the type and age of the waste in each, and the spacing between stacks. For any HTVDD design therefore it is essential to be able to predict the magnitude and spatial distribution of the maximum temperatures attained in and around the disposal.

[107] *Gibb et al.* [2008b] presented a series of case studies for the different versions of VDD/DBD modeled using GRANITE. One of these (case 6) was designed to show how, for HTVDD, the temperature distribution around a stack of containers filled with 76.4% spent PWR fuel pins (45 GWd/t burn up) with a borosilicate glass infill could be controlled simply by choice of the age of the spent fuel in each container within the stack. The case in question modeled a 10 container stack in which 6 containers of 6 year old fuel were flanked, top and bottom, by one container of 25 year old and one of 1.3 year old fuel. Ambient temperature at the bottom of the borehole was taken as 100°C. Other parameters used in this case are reproduced in Table 2. The modeling shows that for any point in or around the containers the temperature rises to a maximum before falling due to the thermal decay of the spent fuel. As is to be anticipated, the maximum temperature decreases with radial distance from the vertical axis of the containers while the time taken to attain it increases, Maximum temperatures also decrease in the vertical direction with distance from the mid point of a stack [see *Gibb et al.*, 2008b, Figure 9]. The results of this modeling can also be shown in the form of isotherms of the maximum temperature attained at any point, irrespective of the time (Figure 9). The most significant isotherm is 700°C, the 150 MPa solidus for the host granite *Attrill and Gibb* [2003a]. Inside this isotherm the granite backfill and wall rock will undergo partial melting, to increasingly greater extents with proximity to the containers, while beyond it the rock will remain solid. Eventually, these melts will recrystallize to form the containment sarcophagus. It is obvious from Figure 9 how the shape and thickness of the sarcophagus can be varied by changing the thermal loading of the containers and this and other consequences for HTVDD are discussed by *Gibb et al.* [2008b].

11.4. Effects on Wall Rocks

[108] Some versions of borehole disposal, e.g., HTVDD, must be in igneous or high-grade metamorphic rocks like granite or granitic gneiss but there is no fundamental reason why others should not be in sedimentary formations such as clays and shales. For HTVDD the effects on the host rock beyond the zone of melting and recrystallization are likely to be minor but they are important. Pre-existing fractures will be annealed by sub-solidus recrystallization while further away any fluid-bearing fracture zones are likely to be partly or completely filled by hydrothermal mineralization. While the latter may not lead to hydraulic conductivities as low as the granite itself, they will be many orders of magnitude less than for open fissures. For LTVDD in sedimentary rocks significant low-grade thermal metamorphism may take place in the host rock adjacent to the

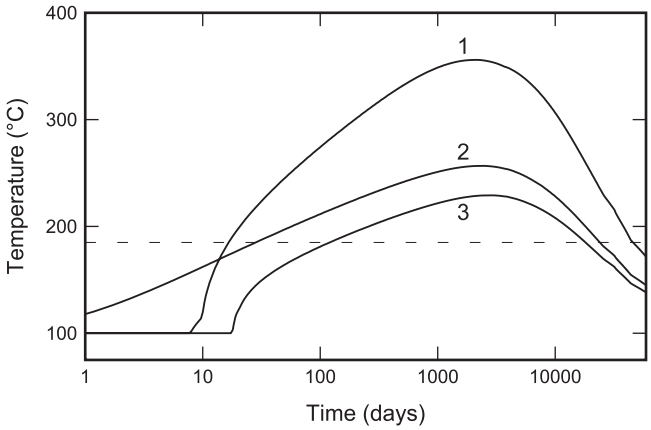

Figure 8. Temperature/time curves for LTVDD-2 of a stack of 10 containers of 30 year old PWR spent fuel (see Table 2 and text). Numbered curves represent points within the high-density support matrix (HDSM) adjacent to the container surface as follows: 1 = mid point of the stack; 2 = bottom of the stack; 3 = top of the stack. The broken horizontal line is the 1 atmosphere solidus of the HDSM. After case A of *Gibb et al.* [2008a].

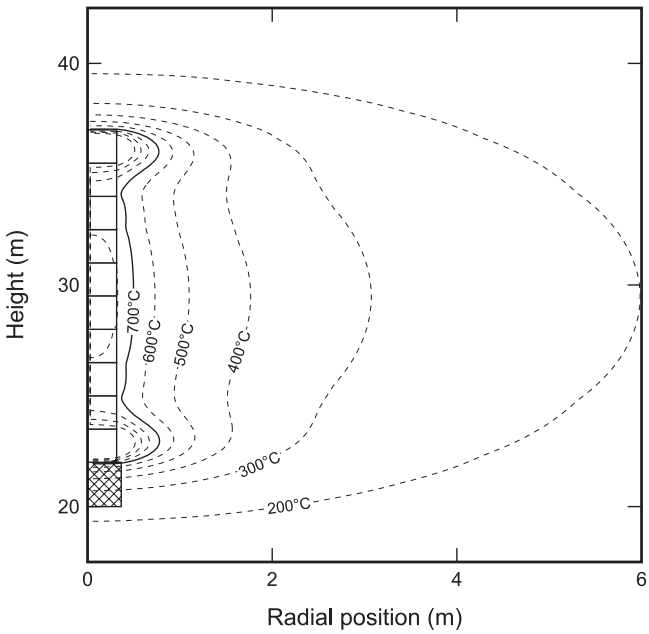

Figure 9. Isotherms of the maximum temperature attained (ambient $T^\circ + \bar{T}$), irrespective of time, for a vertical section through a HTVDD (see text). After case 6 of *Gibb et al.* [2008b].

borehole. Prediction of all of these effects (and any attempts to reproduce them experimentally) requires knowledge of the temperature distribution as provided by the model.

12. Consequences of the Model for Deep Borehole Disposal and Conclusions

[109] Without detailed knowledge of the temperatures reached in and around the waste packages and their changing distribution with time it would be impossible to design a DBD/VDD scheme for any form of heat-generating waste. Each of the many variants of DBD being considered by us and others can only be regarded as viable when the waste form, containers and all components of the scheme can be shown to be capable of performing satisfactorily on the necessary timescale. Temperature is one of the most important parameters in this respect.

[110] The conductive heat flow model described above is generic but flexible enough to accommodate different DBD variants with their different borehole dimensions and designs and a wide range of waste forms, materials etc. Validation of our simulation data against theoretical predictions could only go so far and we acknowledge that our model and computer code reach beyond verifiable boundaries in some respects but we are as confident as we can be that it is fit for purpose.

[111] The model has been used to explore the viability of both low- and high-temperature very deep disposal schemes and to drive modification of the concepts where necessary and several examples of this have already been published elsewhere. It is a key tool for the future of our research into very deep geological disposal and will continue to be developed. Without models and computer codes of this type deep borehole disposal, which is now a serious management option for various high-level waste streams in several countries including the UK, USA and Sweden, could not be progressed.

[112] **Acknowledgments.** We are grateful to Kevin Hesketh and Nexia Solutions for providing the FISPIN data on vitrified waste and spent fuel used to construct the model and for advice on many aspects of high-level wastes and to the (UK) EPSRC for financial support. We also thank Scott Owens for discussion and improvements to the paper and Mike Cooper for drafting the figures.

References

Abramowitz, M., and I. Stegun (1970), *Handbook of Mathematical Functions*, Dover Publications, New York.

Ansolabehere, S., and J. Deutch (2003), *The Future of Nuclear Power: An Interdisciplinary MIT Study*, Massachusetts Institute of Technology, Cambridge, USA.

Attrill, P. G., and F. G. F. Gibb (2003a), Partial melting and recrystallization of granite and their application to deep disposal of radioactive waste, Part 1- Rationale and partial melting, *Lithos*, *67*, 103–117.

Attrill, P. G., and F. G. F. Gibb (2003b), Partial melting and recrystallization of granite and their application to deep disposal of radioactive waste, Part 2- Recrystallization, *Lithos*, *67*, 119–133.

Burstall, R. F. (1979), FISPIN a Computer Code for Nuclide Inventory Calculations, ND-R, 328(R).

Carslaw, H. S., and J. C. Jaeger (1959), *Conduction of Heat in Solids*, 510 pp., Clarendon Press, Oxford.

Chapman, N., and F. Gibb (2003), A truly final waste management solution, *Radwaste Solutions*, *10/4*, 26–37.

Einsenberg, D., and W. Kauzmann (1969), *The Structure and Properties of Water*, 184 pp., Oxford University Press, Oxford.

Gibb, F. G. F. (1999), High-temperature, very deep, geological disposal: A safer alternative for high-level radioactive waste?, *Waste Manage.*, *19*, 207–211.

Gibb, F. G. F. (2000), A new scheme for the very deep geological disposal of high-level radioactive waste, *J. Geol. Soc. London*, *157*, 27–36.

Gibb, F. (2005), Very deep borehole disposal of high-level nuclear waste, *Imperial Eng.*, *3*, 11–13 [Royal School of Mines, Imperial College, London].

Gibb, F. (2006), Retrievability – Safeguard or dangerous illusion?, *Geoscientist*, *16/1*, 14–16.

Gibb, F. G. F., and P. G. Attrill (2003), Granite recrystallization: The key to the nuclear waste problem, *Geology*, *31*, 657–660.

Gibb, F. G. F., N. A. McTaggart, K. P. Travis, D. Burley, and K. W. Hesketh (2008a), High-density support matrices: Key to the deep borehole disposal of spent nuclear fuel, *J. Nucl. Mater.*, *374*, 370–377.

Gibb, F. G. F., K. P. Travis, N. A. McTaggart, D. Burley, and K. W. Hesketh (2008b), Modeling temperature distribution around very deep borehole disposals of HLW, *Nucl. Technol.*, in press.

Harrison, T. (2000), Very deep borehole: Deutag's opinion on boring, container emplacement and retrievability, SKB Report R-00-35, Swedish Nuclear Fuel and Waste Management Co., Stockholm, Sweden.

Hodgkinson, D. P. (1977), *Deep rock disposal of high-level radioactive waste: transient heat conduction from dispersed blocks*, Report R8783, Atomic Energy Research Establishment, Harwell, UK.

Hodgkinson, D. P. (1979), *A mathematical model for hydrothermal convection around a radioactive waste depository in hard rocks*, Report R9149, Atomic Energy Research Establishment, Harwell, UK.

McBirney, A. R. (1984), *Igneous Petrology*, Freeman, San Francisco, USA.

Moller, P., et al. (1997), Paleofluids and recent fluids in the upper continental crust: Results from the German continental deep drilling program (KTB), *J. Geophys. Res.*, *102*(B8), 18,233–18,254.

Press, W. H., S. A. Teukolsky, W. T. Vellerling, and B. P. Flannery (1996), *Numerical Recipes in FORTRAN*, 2e, Cambridge University Press.

Stober, I., and K. Bucher (2004), Fluids within the Earth's crust, *Geofluids*, *4*, 143–151.

Toro, T. (1990), German geology hits new depths, *New Scientist*, 24–25, 29 September.

Vosteen, H.-D., and R. Schellschmidt (2003), Influence of temperature on thermal conductivity, thermal capacity and thermal diffusivity for different types of rock, *Phys. Chem. Earth*, *28*, 499–509.

Whitney, J. A. (1975), The effects of pressure, temperature and X_{H2O} on phase assemblage in four synthetic rock compositions, *J. Geol.*, *83*, 1–31.

Yoder, H. S., Jr. (1976). *Generation of Basaltic Magma*, National Academy of Sciences, Washington DC, USA.

D. Burley, F. G. F. Gibb, N. A. McTaggart, and K. P. Travis, Immobilisation Science Laboratory, Department of Engineering Materials, University of Sheffield, Hadfield Building, Mappin Street, Sheffield, South Yorkshire S1 3JD, UK. (f.gibb@shef.ac.uk)